molecules

MDPI

Article

Synthesis, Antiphospholipase A_2, Antiprotease, Antibacterial Evaluation and Molecular Docking Analysis of Certain Novel Hydrazones

Nahed N. E. El-Sayed [1,2,*], Ahmed M. Alafeefy [3], Mohammed A. Bakht [4], Vijay H. Masand [5], Ali Aldalbahi [6], Nan Chen [7], Chunhai Fan [7] and Abir Ben Bacha [8]

1 Department of Chemistry, College of Science, "Girls Section", King Saud University, P.O. Box 22452, Riyadh 11495, Saudi Arabia
2 National Organization for Drug Control and Research, Giza 35521, Egypt
3 Department of Chemistry, Kulliyyah of Science, International Islamic University, P.O. Box 141, 25710 Kuantan, Malyasia; ahmed.alafeefy@gmail.com
4 Department of Pharmaceutical Chemistry, College of Pharmacy, Prince Sattam Bin Abdulaziz University, P.O. Box 173, Al-kharj 11942, Saudi Arabia; bakhtpharm@gmail.com
5 Department of Chemistry, Vidya Bharati College, Camp, Amravati, Maharashtra 444 602, India; vijaymasand@gmail.com
6 Chemistry Department, King Saud University, P.O. Box 2455, Riyadh 11451, Saudi Arabia; aaldalbahi@ksu.edu.sa
7 Division of Physical Biology & Bioimaging Center, Shanghai Synchrotron Radiation Facility, Shanghai Institute of Applied Physics, Chinese Academy of Sciences, Shanghai 201800, China; chennan@sinap.ac.cn (N.C.); fchh@sinap.ac.cn (C.F.)
8 Biochemistry Department, Science College, King Saud University, P.O. Box 22452, Riyadh 11495, Saudi Arabia; aalghanouchi@ksu.edu.sa
* Correspondence: nelsayed@ksu.edu.sa; Tel.: +966-080-55859

Academic Editor: Derek J. McPhee
Received: 21 October 2016; Accepted: 28 November 2016; Published: 2 December 2016

Abstract: Some novel hydrazone derivatives **6a–o** were synthesized from the key intermediate 4-Chloro-*N*-(2-hydrazinocarbonyl-phenyl)-benzamide **5** and characterized using IR, ^{1}H-NMR, ^{13}C-NMR, mass spectroscopy and elemental analysis. The inhibitory potential against two secretory phospholipase A_2 ($sPLA_2$), three protease enzymes and eleven bacterial strains were evaluated. The results revealed that all compounds showed preferential inhibition towards *h*GIIA isoform of $sPLA_2$ rather than DrG-IB with compounds **6l** and **6e** being the most active. The tested compounds exhibited excellent antiprotease activity against proteinase K and protease from *Bacillus* sp. with compound **6l** being the most active against both enzymes. Furthermore, the maximum zones of inhibition against bacterial growth were exhibited by compounds; **6a**, **6m**, and **6o** against *P. aeruginosa*; **6a**, **6b**, **6d**, **6f**, **6l**, **6m**, **6n**, and **6o** against *Serratia*; **6k** against *S. mutans*; and compounds **6a**, **6d**, **6e**, **6m**, and **6n** against *E. feacalis.* The docking simulations of hydrazones **6a–o** with GIIA $sPLA_2$, proteinase K and hydrazones **6a–e** with glutamine-fructose-6-phosphate transaminase were performed to obtain information regarding the mechanism of action.

Keywords: benzo[*d*][1,3]oxazin-4-one; aroylhydrazides; *N*-acylhydrazones; hydrazones; benzylidene hydrazides; phospholipases; proteases; antimicrobial evaluation; molecular docking

1. Introduction

Hydrazones bearing azomethine moiety can be formed by condensation of hydrazides or aroyl hydrazides with aldehydes [1–4]. These compounds are most widely used as building blocks for the synthesis of 3-acetyl-2,5-disubstituted-2,3-dihydro-1,3,4-oxadiazoles [5], different mono-, di- and

trisubstituted hydrazines [6,7], azetidin-2-ones, thiazolidin-4-ones and methyl thiazolidines [8,9], and formazan derivatives [10,11]. Hydrazones are well known to exhibit a wide spectrum of biological activities [12] and have been utilized as useful candidates for development of antimalarial [13], antitumor [14], antiviral [15,16], antimicrobial [17], antioxidant [18], analgesic, anti-inflammatory and anti-ulcerogenic agents [19,20].

Secreted phospholipases A_2 (sPLA$_2$s) are enzymes found in mammals and animal venoms that catalyze hydrolysis of glycerophospholipids at the *sn*-2 ester position to release a free fatty acid and a lysophospholipid [21]. Mammalian phospholipases have been categorized into ten groups IB, IIA, IIC, IID, IIE, IIF, III, V, X and XIIA [22,23]. It has been reported that sPLA$_2$s play a key role in a good number of bio-chemical processes, thus, on one the hand, group IB sPLA$_2$ has been proposed to be involved in various physiological and pathophysiological processes such as cellular proliferation, cell migration, hormone release [24] and apoptosis in neuronal cells [25]. In addition, higher levels of this enzyme were detected in the serum of patient with chronic renal failure [26] and acute lung injury [27] compared to healthy controls.

On the other hand, the GIIA sPLA$_2$ has been correlated to inflammatory diseases, which is due to elevated levels of this enzyme were detected in the fluids of patients suffering from various inflammatory diseases such as rheumatoid arthritis [28], acute lung injury-acute respiratory distress syndrome (ALI-ARDS) [29] and pancreatitis-associated adrenal injury in acute necrotizing pancreatitis [30], as well as in various cancers [31]. Therefore, seeking potent and selective inhibitors to this sPLA$_2$ may be considered an effective approach to develop novel anti-inflammatory and antitumor agents.

Proteases or proteinases enzymes are proteolytic enzymes that break down proteins into peptides and amino acids. They are classified into different classes depending on their source and functions [32] such as proteinase K, protease from *Bacillus* and protease-esperase. Biologically, proteases are involved in controlling many biological pathways in the life cycle of human, plants, animals, insects and pathogens such as fungi, bacteria and viruses. Many studies reported their involvement in the pathogenic processes of human diseases such as bleeding disorders [33], inflammation [34], cancer [35], hypertension [36] and AIDS [37]. Therefore, proteases inhibitors' can be considered as targets in drug design for developing therapeutics and prevention of diseases [38].

In continuation to our previous efforts towards synthesis of novel biologically active compounds [39–41], we report herein the synthesis of novel hydrazones **6a**–**o** and evaluation of their phospholipases, proteases and bacterial inhibitory activities. The docking simulations of hydrazones **6a**–**o** against GIIA sPLA$_2$, proteinase K and hydrazones **6a**–**e** against glutamine-fructose-6-phosphate transaminase were performed in order to obtain information regarding the mechanism of action.

2. Results and Discussion

2.1. Chemistry

Benzoylation of anthranillic acid **1** with 4-chlorobenzoyl chloride **2** in methylene chloride in the presence of triethylamine afforded the corresponding amido acid **3** which upon boiling with excess of acetic anhydride underwent intramolecular cyclization and afforded benzo[*d*][1,3]oxazin-4-one derivative **4**. Nucleophilic attack by the amino group of hydrazine hydrate on the carbonyl group of the latter benzoxazinone, and subsequent ring opening gives the key intermediate 4-Chloro-*N*-(2-hydrazinocarbonyl-phenyl)-benzamide **5**. Condensation of hydrazino derivative **5** with a variety of aromatic aldehydes yielded the desired hydrazones **6a**–**o** (Scheme 1). The structures of these products were confirmed based on their spectral data and elemental analyses. In general, the IR spectra of compounds **6a**–**o** displayed two absorption bands at ν_{max} 3421–3292 cm^{-1}, which are attributed to the two (NH) groups, and two absorption bands at ν_{max} 1684–1657 cm^{-1} due to the two carbonyl groups. In addition, the (C=N) groups appeared around 1598–1579 cm^{-1}. Moreover, the ^{1}H-NMR spectra of these compounds indicated the disappearance of the spectral line due to NH$_2$

group of the starting hydrazide **5** and appearance of two broad singlet signals at δ 12.37–11.08 ppm corresponding to 2NH groups, singlet signals at δ 8.84–8.30 ppm due to the characteristic azomethines' protons (N=CH) in addition to signals attributed to the aliphatic and aromatic protons at the expected chemical shift values. Analogously, the ^{13}C-NMR spectra proved the presence the two C=O groups at δ_C 165.61–163.86 ppm, azomethine carbons' at 151.46–145.10 ppm and the aliphatic and aromatic carbons at the expected chemical shift values. The mass spectra of all of the synthesized compounds revealed the existence of the parent ion peaks. Finally, the C, H, N elemental analyses of all of the synthesized compounds were in agreement with the proposed structures.

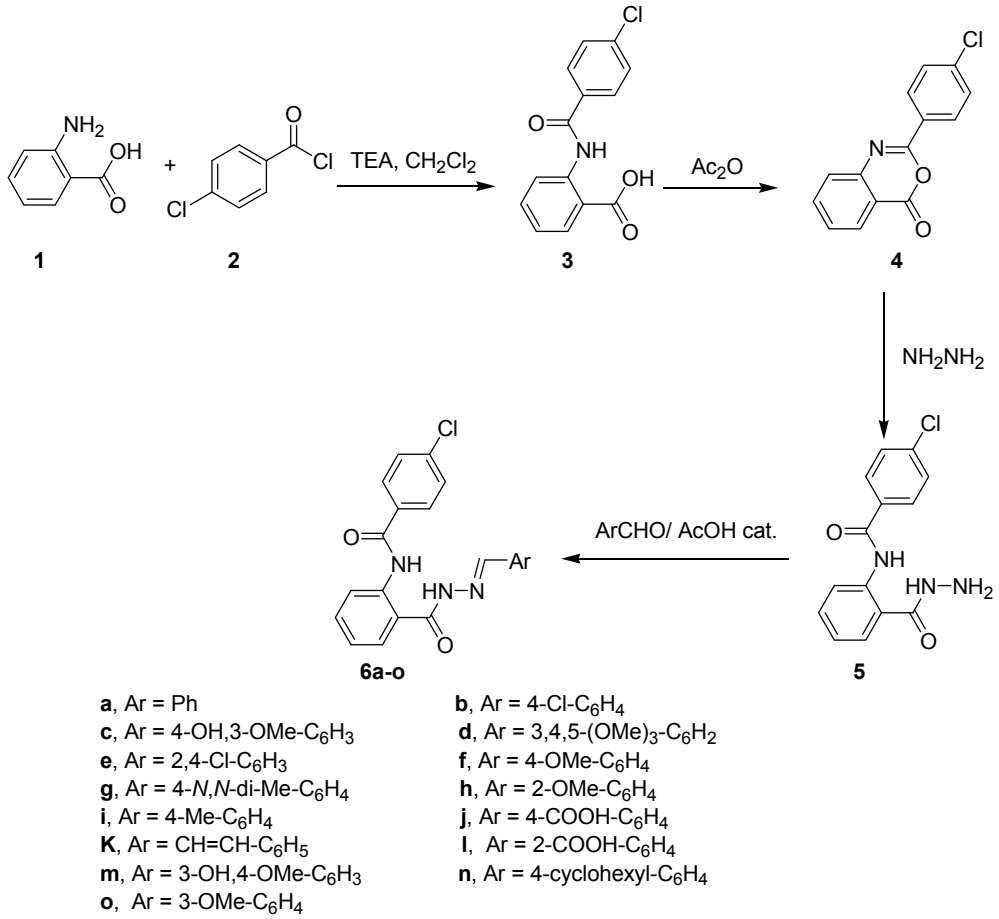

Scheme 1. The synthesis of Schiff bases **6a**–**o**.

2.2. Biological Evaluation

2.2.1. Phospholipases Inhibitory Activity

The phospholipase inhibitory activity of hydrazones **6a**–**o** have been detected against two different classes of sPLA$_2$s, namely human group IIA sPLA$_2$ (hG-IIA) and dromedary group IB sPLA$_2$ (DrG-IB). The obtained results revealed that compounds **6c**, **6d**, **6e** and **6l** exhibited selective inhibition against *h*GIIA rather than DrG-IB by 50.67% ± 4.04%, 55.67% ± 4.72%, 72.67% ± 2.51% and 74.33% ± 3.21%, respectively, as shown in Figure 1 and Table S1.

Conversely, the lowest inhibitory activity against this enzyme (9% ± 2%) was displayed by compound **6n**. These results are in agreement with the data obtained in our previous work [42].

As many clinical studies revealed that the levels of sPLA$_2$s are increased in different inflammatory conditions such as rheumatoid arthritis [28], these active hydrazones can be proposed as potential candidates to explore their utility for such ailment.

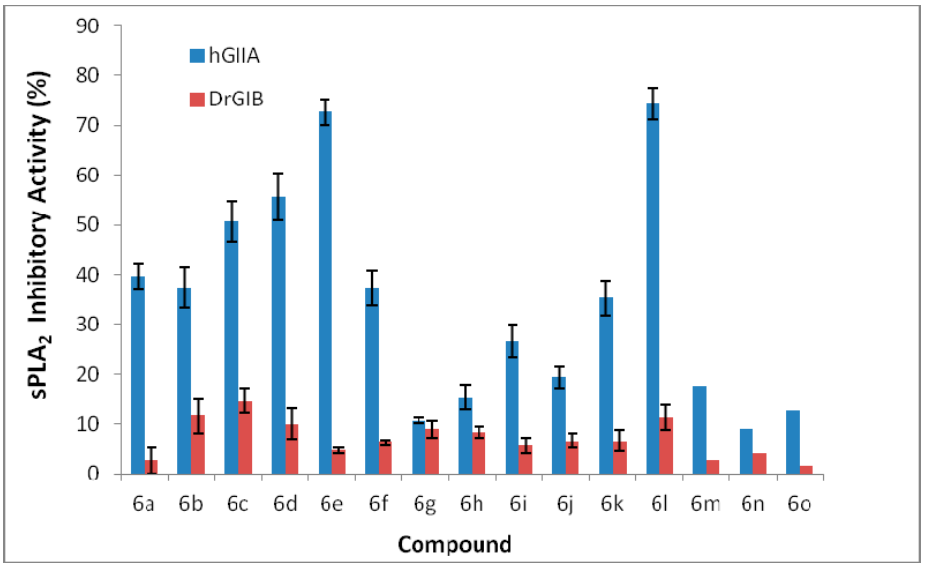

Figure 1. Inhibitory activity (%) of compounds **6a–o** against $sPLA_2$ (hG-IIA and DrG-IB).

2.2.2. Proteases Inhibitory Activity

The synthesized compounds were also screened for in vitro anti-proteases activity against the commercially available protease-esperase, proteinase K and protease obtained from *Bacillus* sp. The screening results shown in Figure 2 and Table S2 revealed that the tested compounds displayed varied degrees of proteases inhibition. The maximum inhibitory activities against proteinase K (86 ± 2.64), protease from *Bacillus* (74.66 ± 2.88) and protease-esperase (39.33 ± 3.21) were exhibited by compound **6l**.

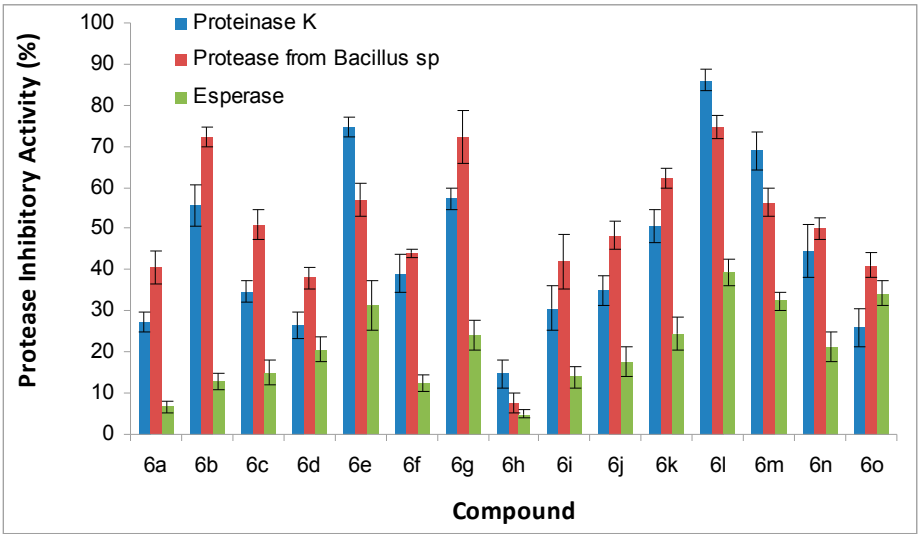

Figure 2. Antiprotease activity (%) of compounds **6a–o** against different protease enzymes.

Furthermore, the next highest inhibitory activities against proteinase K were exhibited by compounds **6e** (74.66% ± 2.51%) and **6m** (69% ± 4.58%), while the next highest inhibitory activities against protease from *Bacillus* sp. were exhibited by compounds **6b** (72.33% ± 2.51%) and **6g** (72.33% ± 6.42%).

It is worth mentioning that most of the compounds showed good antiprotease inhibition against proteinase K and protease from *Bacillus* sp., as depicted in Figure 2. It was also noticed that there was alignment in inhibitory activity against these two enzymes, as any single compound that showed high inhibitory potential against one of them also reacted in a similar fashion towards the other one.

As the anti-inflammatory activities of chemical compounds can be expressed by phospholipase A_2 (hGIIA) and/or through protease inhibitor potentials [42], compound **6l**, which was found to be the most active candidate against both phospholipases A_2 ($sPLA_2$) and protease enzymes under investigation, may be proposed as promising potential anti-inflammatory agent for treatment of ulcerative colitis.

2.2.3. Antibacterial Screening

Finally, compounds **6a**–**o** were further examined for in vitro antibacterial activity. Preliminary screening against eleven strains of Gram-positive and Gram-negative bacteria was performed by adopting standard protocol [43]. The antibacterial potency was determined by measuring the inhibition zones. All tests were performed in duplicates and means of inhibition zones were recorded in mm as presented in Table 1.

Analysis of the screening data revealed that the inhibition activity produced by some of the tested compounds was found to be good to excellent compared to the used reference drug tetracycline. Among the eleven strains that would be considered more susceptible to inhibition by one or more of the synthetic compounds were; *P. aeruginosa*, *Serratia*, *S. aureus*, *S. mutans* and *E. feacalis* with genus *Serratia* being the most sensitive one which was inhibited by nine hydrazones. The highest inhibition towards this pathogen was displayed by compounds **6a**, **6b**, **6d**, **6e**, **6f**, **6l**, **6m**, **6n**, and **6o** with inhibition zones of 15.5 ± 0.0, 12.5 ± 0.0, 12 ± 0.0, 14 ± 1.0, 14 ± 1.0, 13 ± 0.01, 14.5 ± 1.5, 14.5 ± 0.5 and 12.5 ± 0.5, respectively. The highest inhibitory activity against *P. aeruginosa* was exerted by compounds **6a**, **6m**, and **6o** with inhibition zones of 17 ± 1.0, 18.5 ± 0.5 and 18.5 ± 0.5, respectively. Although compounds **6j**, **6l** and **6n** produced the highest inhibition zones against *S. aureus* strain, they were considered to be less effective compared to the reference drug tetracycline. Moreover, the maximum zone of inhibition (24.5 ± 0.5) was exhibited by compound **6k** against *S. mutans*. Finally, the reference drug tetracycline was found to be completely inactive against *E. feacalis*, while compounds **6a**, **6d**, **6e**, **6m**, and **6n** exhibited the maximum inhibition zones of 18.5 ± 0.5, 18.0. ± 1.0, 18.5 ± 0.5, 13.5 ± 1.5 and 18.5 ± 0.5, respectively. The rest of the compounds showed moderate inhibition against all other bacterial strains.

2.3. Molecular Docking Analysis

Based on the data obtained from different biological evaluations, compounds **6a**–**o** were docked against proteinase K, GIIA $sPLA_2$, and compounds **6a**–**e** against glutamine-fructose-6-phosphate transaminase (GlcN6P) synthase (GlmS, L-glutamine: D-fructose-6P amidotransferase, EC 2.6.1.16) in order to provide a conceivable rationale for the observed activities.

2.3.1. Docking Simulations for Compounds **6a**–**o** in Active site of $GIIAsPLA_2$

$GIIAsPLA_2$ is a low molecular weight enzyme (14 kDa) with seven disulfide bonds with a highly conserved Ca^{2+}-binding loop and a catalytic dyad consisting of His47/Asp91 along with active a hydrophobic region lined near the *N*-terminal helix [44].

Table 1. Antibacterial activities of the synthesized hydrazones **6a**–**o**.

Comp #	*Gram-Negative Bacteria*					*Gram-Positive Bacteria*					
	E. coli	***p. aeruginosa***	***K. Pneumoniae***	***Salmonella***	***Serratia***	***S. aureus***	***S. aureus ALA1***	***MRSA ATCC3***	***S. mutans***	***E. feacalis***	***B. subtilis***
6a	0 ± 0	17 ± 1	0 ± 0	8 ± 1	15.5 ± 0	0 ± 0	10 ± 0	12 ± 0	12 ± 0.5	18.5 ± 0.5	0 ± 0
6b	14.5 ± 1.5	12 ± 0	0 ± 0	12.5 ± 0.5	12.5 ± 0.5	8 ± 0.5	0 ± 0	6 ± 0	0 ± 0	9.5 ± 0.5	0 ± 0
6c	1 ± 0	1.5 ± 0	0 ± 0	10.25 ± 1	1.4 ± 1	0 ± 0	0 ± 0	8 ± 0.5	0.6 ± 1.2	1.3 ± 1	0 ± 0
6d	14.5 ± 0.5	10 ± 0	12.2 ± 1	6.5 ± 0	12 ± 0	8.5 ± 0.5	0 ± 0	0 ± 0	10 ± 0.0	18 ± 1	0 ± 0
6e	10 ± 0	12.5 ± 0.1	12.5 ± 0.5	4 ± 0	14 ± 1	8.5 ± 0.5	0 ± 0	14 ± 1	8 ± 1	18.5 ± 0.5	0 ± 0
6f	0 ± 0	10.5 ± 0.1	4.5 ± 0.1	10 ± 0	14 ± 0.1	0 ± 0	0 ± 0	0 ± 0	8 ± 1	0 ± 0	0 ± 0
6g	0 ± 0	10.5 ± 0.5	8 ± 1	0 ± 0	10.5 ± 0.5	8.5 ± 0	0 ± 0	0 ± 0	0 ± 0	0 ± 0	0 ± 0
6h	8 ± 0	12.5 ± 0.7	0 ± 0	0 ± 0	10 ± 0	8.5 ± 0.7	0 ± 0	0 ± 0	0 ± 0	0 ± 0	0 ± 0
6i	8.5 ± 0.5	10.5 ± 0.5	0 ± 0	0 ± 0	8.5 ± 0.5	10.5 ± 1.5	0 ± 0	0 ± 0	0 ± 0	0 ± 0	0 ± 0
6j	8 ± 1	10 ± 0	0 ± 0	0 ± 0	8.5 ± 0.5	19.5 ± 1.5	0 ± 0	0 ± 0	0 ± 0	0 ± 0	0 ± 0
6k	10 ± 0	13.5 ± 1.5	14.5 ± 1.5	0 ± 0	10 ± 0	10.5 ± 1.5	0 ± 0	0 ± 0	24.5 ± 0.5	0 ± 0	8.5 ± 0.5
6l	14 ± 1	11 ± 0	11 ± 0	8 ± 1	13 ± 0.1	18.5 ± 0.5	0 ± 0	0 ± 0	14 ± 2	0 ± 0	0 ± 0
6m	10 ± 1	18.5 ± 0.5	0 ± 0	4 ± 0	14.5 ± 1.5	8.5 ± 0.5	0 ± 0	8.5 ± 0.5	0 ± 0	13.5 ± 1.5	0 ± 0
6n	10 ± 0	0 ± 0	13 ± 1	0 ± 0	12.5 ± 0.5	14 ± 1	0 ± 0	10 ± 0	15 ± 1	18.5 ± 0.5	0 ± 0
6o	10 ± 0	18.5 ± 0.5	10 ± 0	0 ± 0	12.5 ± 0.5	0 ± 0	0 ± 0	0 ± 0	9 ± 0.6	0 ± 0	0 ± 0
TCN	19 ± 0.1	17 ± 0.2	17 ± 0.5	16 ± 0.1	12 ± 0.3	31 ± 0.6	29 ± 0.4	18 ± 0.3	27 ± 1.2	0 ± 0	15 ± 0.5

Comp # = Compound number; TCN = Tetracycline.

The docking simulations for **6a**–**o** in active site of GIIAsPLA$_2$ are presented in Supplementary Materials, Figure S1. Results of docking simulations for compound **6l**, the most active anti-GIIAsPLA$_2$ enzyme, depicted here as a representative in Figure 3, revealed that it interacts with hydrophobic and polar residues of active site of GIIAsPLA$_2$. Compound **6l** has adopted "U" shape with its central benzene ring oriented towards the polar residues viz. His6, Gly22, Asp48, and Val30. The –CONH–N– moiety is responsible for interactions with Phe5 and His47. The –CO–NH–N= moiety bridging the two benzene rings as a polar linker has incorporated good flexibility to the ligand, hence such a flexible moiety is beneficial for further amendments. The –Cl and –COOH groups are oriented toward Leu2 and Val3 due to polar interactions. The –CO– group of –CONH– group is close to Gly22. Hence, –CONH– group is important group for retention in future optimizations.

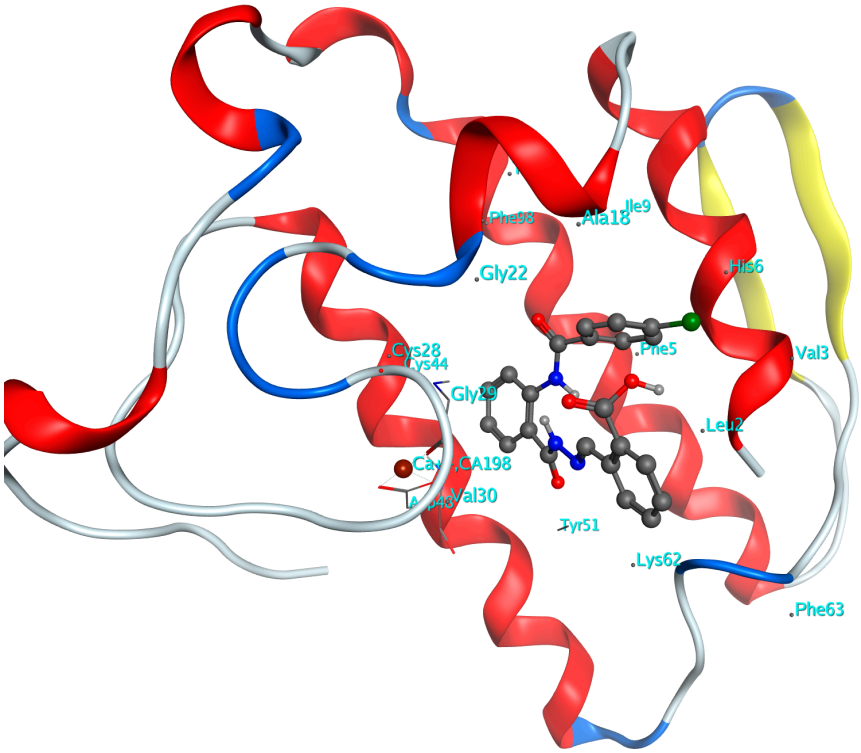

Figure 3. Docking pose for compound **6l** as a representative, in the active site of GIIAsPLA$_2$.

2.3.2. Docking Simulations for Compounds **6a**–**o** in Active Site of Proteinase K

Proteinase K (EC 3.4.21.64, protease K, endopeptidase K, Tritirachium alkaline proteinase, Tritirachium album serine proteinase, and Tritirachium album proteinase K) is a broad-spectrum serine protease belonging to Peptidase family S8 with ability to digest proteins. It is used for the destruction of proteins in cell lysates (tissue, and cell culture cells) and for the release of nucleic acids [45].

The docking simulations for hydrazones **6a**–**o** in active site of proteinase K are presented in Supplementary Materials, Figure S2. Results of docking simulations for compound **6l**, the most active antiproteinase K, depicted here as a representative in Figure 4, revealed that it interacts with hydrophobic and polar residues of active site of proteinase K. Compound **6l** is unable to occupy the complete space of active site of the enzyme. It interacts with polar residues viz. Asn161, Asn162, Ser224 and His69. In addition, it has H-bond formation with H_2O (at distance of 2.86 A°), present inside the active site of Proteinase K, due to the –COOH group present on benzene ring. Hence, the –COOH group is beneficial. Another important interaction is arene-cation interaction between the benzene ring possessing –Cl atom with H_2O (at distance of 4.08 A°), present inside the active site of proteinase K. Interestingly, the compound possesses intramolecular H-bond formation (distance 2.09 A°) between

the –NH– part of –CONH– group with –CO– part of –CONH–N– group. This H-bond is probably responsible for the specific orientation and shape of the molecule inside the active site. The compound **6l** has acquired weird "J" or "L" shape inside the active site. The benzene ring possessing –COOH group is closer to the active site residues. This indicates that the –CONH– and –CONH–N– groups are important for future modifications.

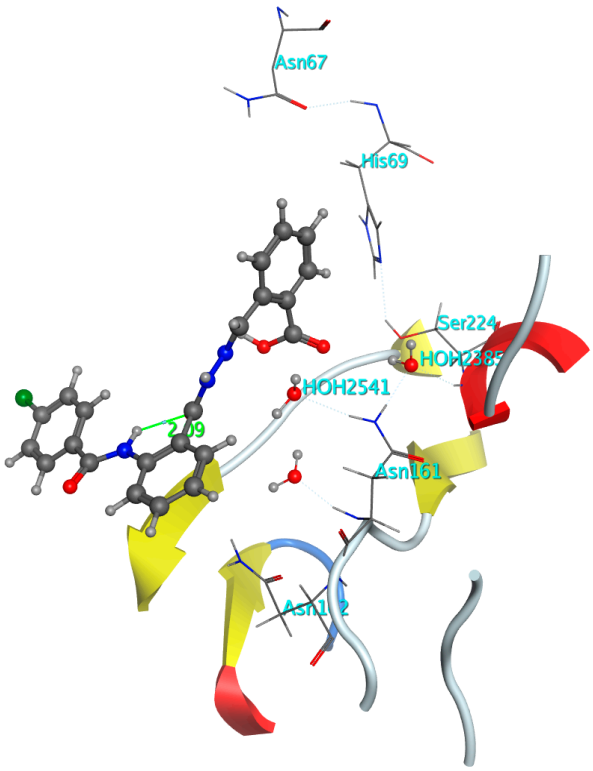

Figure 4. Docking pose for compound **6l** as a representative, in the active site of proteinase K.

2.3.3. Docking Simulations for Compounds **6a–e** in Active Site of Glutamine-Fructose-6-Phosphate Transaminase

The molecular mechanism of multifarious reaction catalyzed by glucosamine-6-phosphate (GlcN6P) synthase (GlmS, L-glutamine: D-fructose-6P amidotransferase, EC 2.6.1.16) enzyme comprises both ammonia transfer (L-glutamine to Fru-6-P) and sugar isomerization (fructosamine-6-phosphate to glucosamine-6-phosphate). This reaction is the initiation of the pathway leading to the eventual production of uridine 5′-diphospho-*N*-acetyl-D-glucosamine (UDP-GlcNAc), a product that is present in all class of organisms, but in fungi and bacteria it is utilized to construct macromolecules essential for the cell wall assembly, such as a number of amino sugar-containing macromolecules, comprising chitin and mannoproteins in fungi, and peptidoglycan and lipopolisaccharides in bacteria. In the prokaryotic cell, the inhibition of GlcN6P synthase even for a small time is fatal. Fortunately, because of the longer lifespan of human, the running down of amino sugar pool for a short time is not deadly. Consequently, it has been proposed as a possible target for developing antibacterial and antifungal agents [46–49].

It is evident that recognition of a molecule by a particular enzyme is dependent on the structural properties of that molecule and its distribution of the molecular electrostatic potential (MEP). Furturmore, analysis of ligand–receptor interactions for GlcN-6-P synthase revealed that ligands having primary amido groups can form stable hydrogen bonds with the amino acids residues present in the binding site of the fungal enzyme thus they may serve as "anchors" to lock the inhibitor in the binding pocket of the enzyme. In addition, previous structure–activity relationship experiments

revealed that presence of active electrophilic center at a proper position is required for inactivation of the enzyme to take place [49]. By analogy, hydrazones **6a**–**o** having the same structural features represented by two primary amido groups and electrophilic double bond may serve as inhibitors for bacterial GlcN6P synthase. This hypothesis is examined by docking hydrazones **6a**–**e** in the active site of the bacterial enzyme (these results are presented in Supplementary Materials, Figure S3).

Docking simulations for the most active candidate **6a** which inhibits collectively three bacterial strains and exhibiting inhibition zones larger than those produced by the reference drug tetracycline against two bacterial strains, *Serratia* and *E. feacalis*, depicted here as a representative in Figure 5, revealed that it interacts with a good number of residues of active site of glucosamine-6-phosphate (GlcN6P) synthase. It mainly interacts with polar and hydrophobic residues of the active site. It has adopted weird "J" or "L" shape in the active site. The oxygen atoms of the two amide groups are responsible for the formation of H-bonding with the polar residues Ser A401 (distance 2.61 A°), Gln A348 (distance 1.94 A°) and Ser A349 (distance 1.71 A°). Hence, the amide groups are beneficial for future development. The arene-cation interaction of benzene ring of ligand with the polar residue Arg A26 has strengthened the binding of ligand with the receptor. The chlorine atom on the benzene ring of the ligand has hydrophobic interactions with the hydrophobic residues Trp A74, Ala A602 and Val A399 that constitute the lipophilic region of the cavity. The –CO-NH-N– moiety present between the two benzene rings as a polar linker has furnished high flexibility to the ligand, hence such a flexible moiety is advantageous for further modifications. The benzene ring, which is acting as a bridge between the two –CONH– groups, is oriented toward polar region of the active site, which comprises polar residues such as Ser A401, Cys A300, Ser A303, Ser A347, Thr A352, Gln A348 and Ser A349.

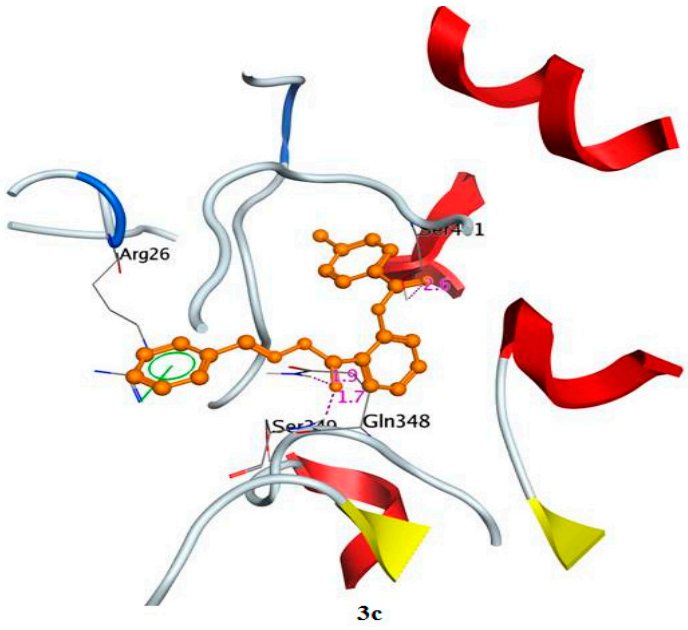

Figure 5. Docking pose for compound **6a**, as a representative, in the active site of glucosamine-6-phosphate (GlcN6P) synthase.

3. Experimental Section

3.1. Chemistry

3.1.1. General

All the chemicals were purchased from various suppliers, and were used without further purification, unless otherwise stated. Melting points were measured on a Gallenkamp melting point

apparatus (Sanyo Gallenkamp, South borough, UK) in open glass capillaries and are uncorrected. Infrared spectra (IR) were recorded using the KBr disc technique using a Perkin Elmer FT-IR spectrophotometer 1000 (PerkinElmer, Waltham, MA, USA). ^{1}H- and ^{13}C-NMR spectra were recorded on a BRUCKER-PLUS NMR (Billerica, MA, USA) operating at 500 MHz in deuterated dimethyl sulfoxide (DMSO-d_6). Chemical shifts are referred to in terms of ppm and *J*-coupling constants are given in Hz. Mass Spectra were recorded on a Shimadzu GCMS-QP 5000 instrument (Shimadzu, Tokyo, Japan). Elemental analysis was done to evaluate the presence of C, H, and N by Perkin Elmer-series-II and the found results were within ±0.4% of the theoretical values. The biological evaluations of the products were carried out at King Saud University, Riyadh, KSA.

3.1.2. Synthetic Procedures

Compounds **3** and **4** were prepared according to reported procedures [20].

4-Chloro-*N*-(2-(hydrazinecarbonyl)phenyl)benzamide **5**

A mixture of 2-(4-chlorophenyl)-4*H*-benzoyl [*d*][1,3]oxazin-4-one **4** (2.57 g, 10 mmol) and 10 mL of hydrazine hydrate (80%) was refluxed for 1 h. Evaporation of the excess hydrazine under reduced pressure and washing of the remaining solid product with plenty of water afford the title compound in pure form.

Yield (95%); shiny white powder; m.p. 175–177 °C. IR (KBr) ν_{max}: 3316–3128 (NH_2 and 2NH), 1673, 1635 (2 C=O), 1592 (C=N) cm^{-1}; ^{1}H-NMR (DMSO-d_6) δ: 12.04 (s, 1H, NHCO), 11.92 (s, 1H, NHCO), 8.51 (d, 1H, Ar-H, *J* = 8.3 Hz), 7.95 (d, 2H, 2 × Ar-H, *J* = 8.4 Hz), 7.90 (d, 1H, Ar-H, *J* = 7.6 Hz), 7.76–7.62 (m, 3H, 3 × Ar-H), 7.28 (t, 1H, Ar-H, *J* = 7.5 Hz), 4.52 (s, 2H, NH_2); ^{13}C-NMR (DMSO-d_6) δ: 165.27 (CO), 164.16 (CO), 138.2, 137.10, 132.43, 129.11, 128.72, 127.80, 125.445, 124.32, 120.93 (12 × Ar-C); MS (ESI): 290 [M^+ + 1], Anal. Calcd. For $C_{14}H_{12}ClN_3O_2$: C (58.04%); H (4.17%); N (14.50%); Found: C (58.08%); H (4.21%); N (14.53%).

Synthesis of Compounds **6a**–**o**

General procedures: A mixture of 4-chloro-*N*-(2-(hydrazinecarbonyl)phenyl)benzamide **5** (2.89 g, 10 mmol) and the appropriate aldehyde (10 mmol) was refluxed in absolute ethanol (15 mL) in presence of few drops of glacial acetic acid as a catalyst for about 4 hour and monitored with TLC (*n*-hexane:EtOAc, 80:20) until the reaction was completed as observed by appearance of a single new spot. The resultant reaction mixture was cooled to room temperature and the solid product obtained in each experiment was collected by filtration and recrystallized from ethanol to afford the desired products **6a**–**o**

N-(2-(2-benzylidenehydrazine-1-carbonyl)phenyl)-4-chlorobenzamide (**6a**) Yield (89%); white crystals; m.p. 244–246 °C; IR (KBr) ν_{max}: 3336–3197 (2 NH), 1673, 1635 (2 C=O), 1592 (C=N) cm^{-1}; ^{1}H-NMR (DMSO-d_6) δ: 12.14 (s, 1H, NHCO), 11.94 (s, 1H, NHCO), 8.51 (d, 1H, Ar-H, *J* = 8.3 Hz), 8.47 (s, 1H, N=CH), 7.96 (d, 2H, 2 × Ar-H, *J* = 8.4 Hz), 7.92 (d, 1H, Ar-H, *J* = 7.6 Hz), 7.76–7.47 (m, 8H, 8 × Ar-H), 7.30 (t, 1H, Ar-H, *J* = 7.5 Hz); ^{13}C-NMR (DMSO-d_6) δ: 165.39 (CO), 164.00 (CO), 149.53 (N=CH), 139.53, 137.42, 134.49, 133.63, 133.06, 130.86, 129.48, 129.36, 129.10, 127.75, 123.85, 121.85, 121.75, 121.31 (18 × Ar-C); MS (ESI): 379 ($C_{21}H_{16}ClN_3O_2$, [M^+ + 1]; Anal. Calcd. for $C_{21}H_{16}ClN_3O_2$: C (66.76%); H (4.27%); N (11.12%); Found: C (66.72%); H (4.24%); N (11.14%).

4-Chloro-N-(2-(2-(4-chlorobenzylidene)hydrazine-1-carbonyl)phenyl)benzamide (**6b**) Yield (95%); white powder; m.p. 252–256 °C; IR (KBr) ν_{max}: 3333–3201 (2 NH), 1675, 1639 (2 C=O), 1598 (C=N) cm^{-1}; ^{1}H-NMR (DMSO-d_6) δ: 12.19 (s, 1H, NHCO), 11.95 (s, 1H, NHCO), 8.52 (d, 1H, Ar-H, *J* = 8.3 Hz), 8.45 (s, 1H, N=CH), 7.96 (d, 2H, 2 × Ar-H, *J* = 8.4 Hz), 7.90 (d, 1H, Ar-H, *J* = 7.8 Hz), 7.77 (d, 2H, 2 × Ar-H, *J* = 8.4 Hz), 7.65–7.61 (m, 3H, 3 × Ar-H), 7.52 (d, 2H, 2 × Ar-H, *J* = 8.4 Hz), 7.28 (t, 1H, Ar-H, *J* = 7.6 Hz); ^{13}C-NMR (DMSO-d_6) δ: 165.46 (CO), 163.96 (CO), 148.13 (N=CH), 139.62, 137.43, 135.32, 133.58, 133.42, 133.10, 129.67, 129.44, 129.33, 129.07, 123.76, 121.71, 121.08 (18 × Ar-C); MS (ESI): 413

[M^+ + 1], Anal. Calcd. for $C_{21}H_{15}Cl_2N_3O_2$: C (61.18%); H (3.67%); N (10.19%); Found: C (61.20%); H (3.64%); N (10.21%).

4-Chloro-N-(2-(2-(4-hydroxy-3-methoxybenzylidene)hydrazine-1-carbonyl)phenyl)benzamide (**6c**) Yield (85%); white crystals; m.p. 236–238 °C; IR (KBr) ν_{max}: 3341–3201 (2 NH and OH), 1675, 1639 (2 C=O), 1588 (C=N) cm^{-1}; ^{1}H-NMR (DMSO-d_6) δ 11.93 (s, 2H, NH and OH), 9.59 (br. s, 1H, NH), 8.46 (d, 1H, Ar-H, *J* = 8.3 Hz), 8.30 (s, 1H, N=CH), 7.90 (d, 2H, 2 × Ar-H, *J* = 8.4 Hz), 7.83 (d, 1H, Ar-H, *J* = 7.7 Hz), 7.58 (d, 2H, 2 × Ar-H, *J* = 8.4 Hz), 7.54 (d, 1H, Ar-H, *J* = 7.7 Hz), 7.29 (d, 1H, Ar-H *J* = 1.0 Hz), 7.21 (t, 1H, Ar-H, *J* = 7.7 Hz), 7.06 (dd, 1H, Ar-H, *J* = 8.1, 1.0 Hz), 6.80 (d, 1H, Ar-H, *J* = 8.1 Hz), 3.78 (s, 3H, OCH_3); ^{13}C-NMR (DMSO-d_6) δ 165.13 (CO), 163.98 (CO), 150.24, 149.81, 148.55, 139.52, 137.41, 133.65, 132.90, 129.46, 129.01, 125.84, 123.78, 123.06, 121.63, 121.31, 115.93, 109.49 (CH=N and 18 × Ar-C), 56.04 (OCH_3); MS (ESI): 425 [M^+ + 1], Anal. Calcd. for $C_{22}H_{18}ClN_3O_4$: C (62.34%); H (4.28%); N (9.91%); Found: C (62.32%); H (4.24%); N (9.93%).

4-Chloro-N-(2-(2-(3,4,5-trimethoxybenzylidene)hydrazine-1-carbonyl)phenyl)benzamide (**6d**) Yield (93%); white crystals; m.p. 247–248 °C; IR (KBr) ν_{max}: 3345–3208 (2 NH), 1671, 1644 (2 C=O), 1578 (C=N) cm^{-1}; ^{1}H-NMR (DMSO-d_6) δ: 12.11 (s, 1H, NHCO), 11.81 (s, 1H, NHCO), 8.46 (d, 1H, Ar-H, *J* = 8.2 Hz), 8.37 (s, 1H, N=CH), 7.96 (d, 2H, 2 × Ar-H, *J* = 8.4 Hz), 7.88 (d, 1H, Ar-H, *J* = 7.6 Hz), 7.67 (d, 2H, 2 × Ar-H, *J* = 8.4 Hz), 7.63 (t, 1H, Ar-H, *J* = 8.2 Hz), 7.31 (t, 1H, Ar-H, *J* = 7.6 Hz), 7.04 (s, 2H, 2 × Ar-H), 3.85 (s, 6H, 2 × OCH_3), 3.74 (s, 3H, OCH_3); ^{13}C-NMR (DMSO-d_6) δ: 165.25 (CO), 164.12 (CO), 153.69 (3 × $\underline{C}$-OCH_3), 146.48 (N=CH), 139.32, 137.39, 133.68, 129.97, 129.52, 129.47, 129.15, 123.96, 121.96, 104.96 (15 × Ar-C), 60.60 (OCH_3), 56.50 (OCH_3), 56.46 (OCH_3). MS (ESI): 469 [M^+ + 1], Anal. Calcd. for $C_{24}H_{22}ClN_3O_5$: C (61.61%); H (4.74%); N (8.98%); Found: C (61.32%); H (4.71%); N (9.02%).

4-Chloro-N-(2-(2-(2,4-dichlorobenzylidene)hydrazine-1-carbonyl)phenyl)benzamide (**6e**) Yield (93%); creamish powder; m.p. 262–264 °C; IR (KBr) ν_{max}: 3421–3268 (2 NH), 1680, 1656 (2 C=O), 1592 (C=N) cm^{-1}; ^{1}H-NMR (DMSO-d_6) δ: 12.36 (s, 1H, NHCO), 11.79 (s, 1H, NHCO), 8.82 (s, 1H, N=CH), 8.47 (d, 1H, Ar-H, *J* = 8.3 Hz), 8.04 (d, 1H, Ar-H, *J* = 8.5 Hz), 7.95 (d, 2H, 2 × Ar-H, *J* = 8.4 Hz), 7.91 (d, 1H, Ar-H, *J* = 7.8 Hz), 7.75 (s, 1H, CH-Ar), 7.69–7.64 (m, 3H, 3 × Ar-H), 7.55 (d, 1H, Ar-H, *J* = 8.5 Hz), 7.31 (t, 1H, Ar-H, *J* = 7.6 Hz); ^{13}C-NMR (DMSO-d_6) δ: 165.31 (CO), 164.42 (CO), 148.38 (N=CH), 139.64, 137.93, 135.26, 133.45, 133.39, 133.10, 129.51, 129.49, 129.27, 129.11, 123.80, 121.71, 121.88 (18 × Ar-C). MS (ESI): 447 [M^+ + 1], Anal. Calcd. for $C_{21}H_{14}Cl_3N_3O_2$: C (56.46%); H (3.16%); N (9.41%); Found: C (56.48%); H (3.20%); N (9.42%).

4-Chloro-N-[2-(4-methoxy-benzylidene-hydrazinocarbonyl)-phenyl]-benzamide (**6f**) Yield (88%); white powder; m.p. 260–262 °C; IR (KBr) v_{max}: 3374–3242 (2 NH), 1682, 1646 (2 C=O), 1589 (C=N) cm^{-1}; ^{1}H-NMR (DMSO-d_6) δ: 12.06 (s, 1H, NHCO), 12.03 (s, 1H, NHCO), 8.55 (d, 1H, Ar-H, *J* = 8.3 Hz), 8.42 (s, 1H, CH=N), 7.96 (d, 2H, 2 × Ar-H, *J* = 8.5 Hz), 7.91 (d, 1H, Ar-H, *J* = 7.6 Hz), 7.69 (d, 2H, 2 × Ar-H, *J* = 8.7 Hz), 7.64 (d, 2H, 2 × Ar-H, *J* = 8.5 Hz), 7.60 (t, 1H, Ar-H, *J* = 7.5 Hz), 7.27 (t, 1H, Ar-H, *J* = 7.5 Hz), 7.02 (d, 2H, 2 × Ar-H, *J* = 8.7 Hz), 3.80 (s, 3H, OCH_3); ^{13}C-NMR (DMSO-d_6) δ: 165.25 (CO), 163.91 (CO), 161.55 ($\underline{C}$-OCH_3), 149.54 (N=CH), 139.65, 137.42, 133.60, 132.96, 129.45, 129.42, 128.99, 127.01, 123.69, 121.53, 121.02, 114.82 (17 × Ar-C), 55.75 (OCH_3). MS (ESI): 409 [M^+ + 1], Anal. Calcd. for $C_{22}H_{18}ClN_3O_3$: C (64.79%); H (4.45%); N (10.30%); Found: C (64.78%); H (4.42%); N (10.32%).

4-Chloro-N-(2-(2-(4-(dimethylamino)benzylidene)hydrazine-1-carbonyl)phenyl)benzamide (**6g**) Yield (82%); yellow powder; m.p. 249–251 °C; IR (KBr) ν_{max}: 3364–3212 ((2 NH), 1679, 1640 (2 C=O), 1582 (C=N) cm^{-1}; ^{1}H-NMR (DMSO-d_6) δ: 12.11 (s, 1H, NHCO), 11.85 (s, 1H, NHCO), 8.56 (d, 1H, Ar-H, *J* = 8.2 Hz), 8.32 (s, 1H, CH=N), 7.96 (d, 2H, 2 × Ar-H, *J* = 8.5 Hz), 7.90 (d, 1H, Ar-H, *J* = 7.2 Hz), 7.68 (d, 2H, 2 × Ar-H, *J* = 8.5 Hz), 7.62 (t, 1H, Ar-H, *J* = 7.4 Hz), 7.56 (d, 2H, 2 × Ar-H, *J* = 8.8 Hz), 7.28 (t, 1H, Ar-H, *J* = 7.4 Hz), 6.77 (d, 2H, 2 × Ar-H, *J* = 8.8 Hz), 2.99 (s, 6H, 2 × N-CH_3); ^{13}C-NMR (DMSO-d_6) δ: 165.31 (CO), 164.13 (CO), 152.4 ($\underline{C}$-NCH_3), 148.27 (N=CH), 138.2, 137.4, 134.84, 129.53, 129.44, 129.18, 128.8, 127.7, 124.2, 123.74, 119.8, 112.3 (17 × Ar-C), 45.2 (2 × CH_3). MS (ESI): 422 [M^+ + 1], Anal. Calcd. for $C_{23}H_{21}ClN_4O_2$: C (65.63%); H (5.03%); N (13.31%); Found: C (65.59%); H (5.02%); N (13.33%).

4-Chloro-N-(2-(2-(2-methoxybenzylidene)hydrazine-1-carbonyl)phenyl)benzamide (**6h**) Yield (98%); white powder; m.p. 236–238 °C; IR (KBr) ν_{max}: 3383–3251 ((2 NH), 1680, 1652 (2 C=O), 1589 (C=N) cm^{-1}; ^{1}H-NMR (DMSO-d_6) δ: 12.06 (s, 1H, NHCO), 11.97 (s, 1H, NHCO), 8.77 (s, 1H, N=CH), 8.47 (d, 1H, Ar-H, *J* = 8.3 Hz), 7.90 (d, 2H, 2 × Ar-H, *J* = 8.5 Hz), 7.88–7.83 (m, 2H, 2 × Ar-H), 7.60 (d, 2H, 2 × Ar-H, *J* = 8.5 Hz), 7.58–7.20 (m, 3H, 3 × Ar-H, *J* = 7.5 Hz), 7.05 (d, 1H, Ar-H, *J* = 8.4 Hz), 6.98 (t, 1H, Ar-H, *J* = 7.7 Hz), 3.80 (s, 3H, O-CH_3); ^{13}C-NMR (DMSO-d_6) δ: 165.28 (CO), 163.96 (CO), 158.39 (C-OCH_3), 145.11 (N=CH), 139.63, 137.42, 133.64, 133.05, 132.40, 129.49, 129.46, 129.09, 126.09, 123.77, 122.47, 121.58, 121.23, 120.99, 112.37 (17 × Ar-C), 56.18 (OCH_3). MS (ESI): 409 [M^+ + 1], Anal. Calcd. for $C_{22}H_{18}ClN_3O_3$: C (64.79%); H (4.45%); N (10.30%); Found: C (64.82%); H (4.46%); N (10.33%).

4-Chloro-N-(2-(2-(4-methylbenzylidene)hydrazine-1-carbonyl)phenyl)benzamide (**6i**) Yield (91%); white crystals; m.p. 256–258 °C; IR (KBr) ν_{max}: 3372-3264 ((2 NH), 1684, 1657 (2 C=O), 1579 (C=N) cm^{-1}; ^{1}H-NMR (DMSO-d_6) δ: 12.08 (s, 1H, NHCO), 11.97 (s, 1H, NHCO), 8.52 (d, 1H, Ar-H, *J* = 8.3 Hz), 8.43 (s, 1H, N=CH), 7.98 (d, 1H, Ar-H, *J* = 8.5 Hz), 7.91 (d, 2H, 2 × Ar-H, *J* = 7.7 Hz), 8.68–7.62 (m, 5H, 5 × Ar-H), 7.31–7.28 (m, 3H, 3 × Ar-H), 2.34 (s, 3H, CH_3); ^{13}C-NMR (DMSO-d_6) δ (ppm): 165.31 (CO), 163.98 (CO), 149.61 (N=CH), 140.77, 139.55, 137.42, 133.62, 133.62, 133.02, 131.78, 129.97, 129.49, 129.46, 129.06, 127.74, 123.81, 121.67, 121.24 (18 × Ar-C), 21.52 (CH_3). MS (ESI): 393 [M^+ + 1], Anal. Calcd. for $C_{22}H_{18}ClN_3O_2$: C (67.43%); H (4.63%); N (10.72%); Found: C (64.42%); H (4.66%); N (10.73%).

4-((2-(2-(4-chlorobenzamido)benzoyl)hydrazono)methyl)benzoic acid (**6j**) Yield (85%); creamish powder; m.p. 252–254 °C; IR (KBr) ν_{max}: 3373–3292 (2 NH, OH), 1759, 1680, 1652 (3 C=O), 1581 (C=N) cm^{-1}; ^{1}H-NMR (DMSO-d_6) δ: 12.25 (s, 1H, NHCO), 11.92 (s, 1H, NHCO), 8.51 (s, 1H, N=CH), 8.04–7.25 (m, 12H, 12 × Ar-H); ^{13}C-NMR (DMSO-d_6) δ: 167.37 (COOH), 165.58 (CONH), 163.98 (CO), 148.24 (N=CH), 139.63, 138.49, 137.44, 133.56, 133.13, 132.42, 130.26, 129.40, 129.30, 129.09, 127.72, 123.75, 121.75, 121.05 (18 × Ar-C). MS: *m*/*z* 423 [M^+ + 1], Anal. Calcd. for $C_{22}H_{16}ClN_3O_4$: C (62.64%); H (3.82%); N (9.96%); Found: C (62.63%); H (3.86%); N (9.97%).

Chloro-N-(2-(2-(3-phenylallylidene)hydrazine-1-carbonyl)phenyl)benzamide (**6k**) Yield (93%); creamish powder; m.p. 248–250 °C; IR (KBr) ν_{max}: 3391–3271 (2 NH), 1680, 1644 (2 C=O), 1594 (C=N) cm^{-1}; ^{1}H-NMR (DMSO-d_6) δ: 12.04 (s, 1H, NHCO), 11.97 (s, 1H, NHCO), 8.51 (d, 1H, Ar-H, *J* = 7.8 Hz), 8.25 (d, 1H, N=CH, *J* = 8.3 Hz), 7.95 (d, 2H, 2 × Ar-H, *J* = 8.5 Hz), 7.88 (d, 1H, *J* = 7.8 Hz, Ar-H), 7.68 (d, 2H, 2 × Ar-H, *J* = 8.5 Hz), 7.64–7.62 (m, 3H, 3 × Ar-H, *J* = 7.6 Hz), 7.41 (t, 2H, 2 × Ar-H, *J* = 7.3 Hz), 7.36–7.08 (m, 4H, 4 × Ar-H); ^{13}C-NMR (DMSO-d_6) δ: 165.29 (CO), 163.92 (CO), 151.46, 140.39, 139.49, 137.44, 136.26, 129.50, 129.45, 129.34, 129.05, 127.67, 125.84, 123.84, 121.28 (N=C<u>H</u>-C<u>H</u>=C<u>H</u> and 18 × Ar-C). MS: *m*/*z* 405 [M^+ + 1], Anal. Calcd. for $C_{23}H_{18}ClN_3O_2$: C (68.40%); H (4.49%); N (10.40%); Found: C (68.42%); H (4.51%); N (10.44%).

2-((2-(2-(4-chlorobenzamido)benzoyl)hydrazono)methyl)benzoic acid (**6l**) Yield (87%); white powder; m.p. 251–253 °C; IR (KBr) ν_{max}: 3368–3278 (2 NH and OH), 1758 (CO), 1680, 1656 (2 C=O), 1579 (C=N) cm^{-1}; ^{1}H-NMR (DMSO-d_6) δ: 12.37 (s, 1H, NHCO), 11.95 (s, 1H, NHCO), 8.74 (s, 1H, N=CH), 8.52 (d, 1H, Ar-H, *J* = 8.3 Hz), 8.09 (d, 1H, Ar-H, *J* = 7.8 Hz) 7.97 (d, 2H, 2 × Ar-H, *J* = 8.5 Hz), 7.95–7.62 (m, 6H, 6 × Ar-H), 7.56 (t, 1H, Ar-H, *J* = 7.4 Hz), 7.28 (t, 1H, Ar-H, *J* = 7.4 Hz); ^{13}C-NMR (DMSO-d_6) δ: 168.51 (COOH), 165.61 (CO), 164.02 (CO), 148.38 (N=CH), 139.56, 137.39, 134.82, 133.66, 133.09, 132.49, 131.29, 130.35, 129.47, 129.25, 127.23, 123.78, 121.70, 121.19 (18 × Ar-C). MS (ESI): 423 [M^+ + 1], Anal. Calcd. for $C_{22}H_{16}ClN_3O_4$: C (62.64%); H (3.82%); N (9.96%); Found: C (62.67%); H (3.85%); N (9.88%).

4-Chloro-N-(2-(2-(3-hydroxy-4-methoxybenzylidene)hydrazine-1-carbonyl)phenyl)benzamide (**6m**) Yield (94%); white powder; m.p. 239–241 °C; IR (KBr) ν_{max}: 3383–3256 (2 NH), 1680, 1657 (2 C=O), 1582 (C=N) cm^{-1}; ^{1}H-NMR (DMSO-d_6) δ: 12.04 (s, 1H, NHCO), 11.97 (s, 1H, NHCO), 8.56 (d, 1H, Ar-H, *J* = 8.3 Hz), 8.34 (s, 1H, N=CH), 7.96 (d, 2H, 2 × Ar-H, *J* = 8.5 Hz), 7.90 (d, 1H, *J* = 7.7 Hz), 7.67 (d, 2H, 2 × Ar-H, *J* = 8.5 Hz), 7.62 (t, 1H, Ar-H, *J* = 7.5 Hz), 7.31 (d, 1H, Ar-H, *J* = 1.6 Hz), 7.28 (t, 1H, Ar-H, *J* = 7.6 Hz), 7.08 (dd, 1H, Ar-H, *J* = 8.3, 1.6 Hz), 6.98 (d, 1H, Ar-H, *J* = 8.3 Hz), 3.82 (s, 3H, O-CH_3); ^{13}C-NMR (DMSO-d_6) δ: 165.16 (CO), 163.93 (CO), 150.53, (C-OCH_3), 149.81 (C-OH), 147.37 (N=CH),

139.58, 137.44, 133.62, 132.62, 129.49, 129.43, 129.01, 127.29, 123.77, 121.55, 121.13, 112.90, 112.29 (16 × Ar-C), 56.04 (OCH_3). MS (ESI): 425 [M^+ + 1], Anal. Calcd. for $C_{22}H_{18}ClN_3O_4$: C (62.34%); H (4.28%); N 00(9.91%); Found: C (62.38%); H (4.26%); N (9.93%).

4-Chloro-N-(2-(2-(4-cyclohexylbenzylidene)hydrazine-1-carbonyl)phenyl)benzamide (**6n**) Yield (85%); white crystals; m.p. 257–259 °C; IR (KBr) ν_{max}: 3386–3260 (2 NH), 1682, 1654 (2 C=O), 1589 (C=N) cm^{-1}; ^{1}H-NMR (DMSO-d_6) δ: 12.03 (s, 1H, NHCO), 11.08 (s, 1H, NHCO), 8.51 (d, 1H, Ar-H, *J* = 8.2 Hz), 8.36 (s, 1H, N=CH), 7.95 (d, 2H, 2 × Ar-H, *J* = 8.5 Hz), 7.88 (d, 1H, Ar-H, *J* = 7.7 Hz), 7.65 (d, 2H, 2 × Ar-H, *J* = 8.3 Hz), 7.59 (t, 1H, Ar-H, *J* = 7. 7Hz), 7.31–7.18 (m, 5H, 5 × Ar-H), 3.09–1.55 (m, 11H, cyclohexyl-H); ^{13}C-NMR (DMSO-d_6) δ: 165.54 (CO), 163.86 (CO), 146.14 (N=CH), 139.23, 137.44, 133.55, 132.61, 129.47, 129.39, 128.84, 127.16, 126.60, 123.76, 121.72, 121.49 (18 × Ar-C), 42.85, 41.23, 35.32, 34.39, 33.43, 28.39 (cyclohexyl-C). MS (ESI): 461 [M^+ + 1], Anal. Calcd. For $C_{27}H_{26}ClN_3O_2$: C (70.50%); H (5.70%); N (9.14%); Found: C (70.51%); H (5.71%); N (9.13%).

(Z)-4-chloro-N-(2-(2-(3-hydroxybenzylidene)hydrazine-1-carbonyl)phenyl)benzamide (**6o**) Yield (95%); white powder; m.p. 262–264 °C; IR (KBr) ν_{max}: 3386–3258 (2 NH, OH), 1680, 1652 (2 C=O), 1579 (C=N) cm^{-1}; ^{1}H-NMR (DMSO-d_6) δ: 12.12 (s, 1H, NHCO), 12.04 (s, 1H, NHCO), 8.84 (s, 1H, N=CH), 8.55 (d, 1H, Ar-H, *J* = 8.3 Hz), 7.97 (d, 2H, 2 × Ar-H, *J* = 8.5 Hz), 7.95–7.90 (m, 2H, 2 × Ar-H), 7.67 (d, 2H, 2 × Ar-H, *J* = 8.5 Hz), 7.63 (t, 1H, Ar-H, *J* = 7.5 Hz), 7.46–7.03 (m, 4H, 4 × Ar-H); ^{13}C-NMR (DMSO-d_6) δ: 165.27 (CO), 163.96 (CO), 158.40 (C-OCH_3), 145.10 (N=CH), 139.64, 137.42, 133.64, 133.05, 132.40, 129.50, 129.46, 129.09, 126.09, 123.77, 122.47, 121.48, 121.57, 121.23, 120.99 (17 × Ar-C). MS (ESI): 395 [M^+ + 1], Anal. Calcd. For $C_{21}H_{16}ClN_3O_3$: C (64.05%); H (4.09%); N (10.67%); Found: C (64.07%); H (4.12%); N (10.63%).

3.2. Biological Evalustion

3.2.1. Inhibition of $sPLA_2$ Activity

The test of inhibitory activity of secretory phospholipase A_2 ($sPLA_2$) was performed as described by De Aranjo and Radvany [50]. Briefly, the substrate consisted of 3.5 mM lecithin in a mixture of 3 mM NaTDC, 100 mM NaCl, 10 mM $CaCl_2$ and 0.055 mM red phenol as colorimetric indicator in 100 mL H_2O. The pH of the reaction mixture was adjusted to 7.6 using phosphate buffer. The Human group IIA (hG-IIA) and dromedary group IB (DrG-IIA) $sPLA_2$ were solubilized in 10% acetonitrile at a concentration of 0.05 μg/μL. A volume of 10 μL of these PLA_2 solutions was incubated with 10 μL containing 10 μg of each compound for 20 min at room temperature. Then, 1 mL of the PLA_2 substrate was added, and the kinetic of hydrolysis was followed during 5 min by reading the optical density at 558 nm. The inhibition percentage was calculated by comparison with a control experiment (absence of compound).

3.2.2. Protease Inhibitor Assay

Three commercially available proteases; proteinase K (Sigma-Aldrich, St. Louis, MO, USA, P2308), esperase (Novozyme, Sigma-Aldrich, P5860) and that obtained from *Bacillus* sp. (Sigma-Aldrich, P3111) were evaluated for the effect of the studied compounds on their activities. Protease assays were carried out by adopting Kunitz caseinolytic method [51] using Hammerstein casein as substrate. Respective protease inhibitor activities were assayed under the same conditions with the addition of the inhibitor (0.1 mg/mL) to the respective reaction mixture and pre incubation for 10 min at 37 °C. The assay of the residual enzyme activity was followed by the addition of 2 mL of 1% casein and the resulting mixture was allowed to stand for 30 min at 37 °C. The reaction was stopped by the addition of 2.5 mL of 5% TCA solution. After centrifugation of the reaction mixture (12,000 rpm, 15 min), the absorbance was measured at 280 nm. Protease inhibitor unit is defined as the amount of protease inhibitor that inhibited one unit of respective enzyme activity. The protease inhibitor activity was expressed in

terms of percent inhibition. Appropriate blanks for the enzyme, inhibitor, and the substrate were also included in the assay along with the test.

3.2.3. Antibacterial Activity

Culture of Microbial Strains Preparation

Pure standard microbial isolates collected from King Khaled University Hospital were tested in this study; including *Staphylococcus aureus* ATCC 25923, Methicillin resistant *Staphylococus aureus* ATCC 12498, *Bacillus subtilis* ATCC 6633, *Enterococcus faecalis* ATCC 29212 as Gram-positive and *Escherichia coli* ATCC 25966, *Pseudomonas aeruginosa* ATCC 27853 and *Serratia marcescens* as Gram-negative bacteria. Fresh cultures of each microorganism were grown on nutrient agar plates (Oxoid, Thermo Scientific, Basingstoke, UK); of which small inoculums were suspended in 5 mL nutrient broth for bacterial suspension preparation of 0.5 MacFarland.

Antibacterial Assay

Antimicrobial activity was assayed using well diffusion technique according to given literature [43]. Briefly, small inoculums of each of the microbial suspension prepared were loaded on sterile Muller Hinton agar plates surface (Oxoid) with sterile cotton swabs. Loaded plates were then perforated equidistantly with a sterile 6 mm diameter cork borer, and 70 µL of each compound solution (1 mg/mL) were loaded in their respective wells. DMSO and Tetracycline were used as negative and positive controls, respectively. Plates were kept to rest for 30 min at room temperature and then incubated at 37 °C for 18–24 h. Antimicrobial activity was determined by measuring the inhibition zone. All tests were performed in duplicates and means of inhibition zones were recorded in mm.

3.3. Molecular Docking

In the present work, AutoDock 4.0 (The Scripps Research Institute, La Jolla, CA, USA) was used for molecular docking. The software is freely available and can be used with different molecular viewers like PMV, PyMol, etc. For docking simulations, the structures of the molecules were drawn using ChemSketch 12.0 (Advanced Chemistry Development, Inc., Toronto, ON, Canada) freeware and optimized using the inbuilt methodology. The optimized structures were saved in 3D-format in .mol file format. The structures of proteins GIIA $sPLA_2$ (pdb: 1DB4), proteinase K (pdb: 2PWB) and glutamine-fructose-6-phosphate transaminase (1JXA) were retrieved from www.rcsb.org. The pdb 1DB4, 2PWB, and 1JXA for the proteins were selected on the basis of reasonable X-ray resolution and sequence completion. The proteins structures were optimized before actual docking simulations. Following parameters were set for getting better docking results: Algorithm: genetic Algorithm; Number of runs: 10 GA runs; Number of evaluations: 250,000 evaluation/run; population size: 150.

4. Conclusions

In conclusion, fifteen novel hydrazone derivatives **6a–o** were synthesized, fully characterized and examined to evaluate their inhibitory activity against two phospholipases A_2, three protease enzymes and a panel of Gram-negative and Gram-positive bacterial strains. Among the investigated compounds; **6e** and **6l** selectively exhibited $sPLA_2$ the highest inhibitory activity against *h*G-IIA isoform. It is quite interesting to report that compound **6l** also displayed the highest antiprotease inhibition against all used protease enzymes.

Moreover, the series under investigation showed varied antibacterial inhibitory activity. Thus, while similar inhibition to that produced by the reference drug tetracycline was displayed by compound **6a** against *P. aeruginosa*, compounds **6m** and **6o** exhibited higher inhibition. In addition, the most susceptible bacterial strain to the synthesized compounds was genus *Serratia*, which was inhibited by nine of them, with compound **6a** being the most powerful inhibitory agent. Furthermore, the maximum inhibitory activities were exhibited by compounds **6j**, **6l**, and **6n** against *S. aureus* and by compound

6k against *S. mutans*. Finally, compounds **6a**, **6d**, **6e**, **6m** and **6n** were found to be more potent than the used reference drug against *E. feacalis*. The docking simulations of compounds **6a–o** with GIIA $sPLA_2$, proteinase K and compounds **6a–e** GlcN6P were carried out in order to investigate the mode of action.

Supplementary Materials: Supplementary materials can be accessed at: http://www.mdpi.com/1420-3049/21/12/1664/s1.

Acknowledgments: The authors are thankful to "The Visiting Professor Program at King Saud University".

Author Contributions: Nahed N. E. El-Sayed and Ahmed M. Alafeefy conceived, designed the experiments, analyzed the spectral data and wrote the manuscript; Mohammaed A. Bakht performed the experiments; Vijay H. Masand performed the docking studies; Abir Ben Bacha performed the biological studies; and Ali Aldalbahi, Nan Chen and Chunhai Fan helped in discussion.

Conflicts of Interest: The authors declare no conflict of interest.

References

1. Miklos, F.; Fulop, F. A Simple Green Protocol for the Condensation of Anthranilic Hydrazide with Cyclohexanone and *N*-Benzylpiperidinone in Water. *J. Heterocycl. Chem.* **2016**, *53*, 32–37. [CrossRef]
2. Jamil, W.; Perveen, S.; Shah, S.A.A.; Taha, M.; Ismail, N.H.; Perveen, S.; Ambreen, N.; Khan, K.M.; Choudhary, M.I. Phenoxyacetohydrazide Schiff Bases: β-Glucuronidase Inhibitors. *Molecules* **2014**, *19*, 8788–8802. [CrossRef] [PubMed]
3. Wang, L.; Guo, D.G.; Wang, Y.Y.; Zheng, C.Z. 4-Hydroxy-3-methoxy-benzaldehyde series aroyl hydrazones: Synthesis, thermostability and antimicrobial activities. *RSC Adv.* **2014**, *4*, 58895–58901. [CrossRef]
4. Ienascu, I.M.C.; Lupea, A.X.; Popescu, I.M.; Padure, M.A.; Zamfir, A.D. The synthesis and characterization of some novel 5-chloro-2-(substituted alkoxy)-*N*-phenylbenzamide derivatives. *J. Serbian Chem. Soc.* **2009**, *74*, 847–855. [CrossRef]
5. Jin, L.; Chen, J.; Song, B.; Chen, Z.; Yang, S.; Li, Q.; Hu, D.; Xu, R. Synthesis, structure, and bioactivity of *N*′-substituted benzylidene-3,4,5-trimethoxybenzohydrazide and 3-acetyl-2-substituted phenyl-5-(3,4,5-trimethoxyphenyl)- 2,3-dihydro-1,3,4-oxadiazole derivatives. *Bioorg. Med. Chem. Lett.* **2006**, *16*, 5036–5040. [CrossRef] [PubMed]
6. Perdicchia, D.; Licandro, E.; Maiorana, S.; Baldoli, C.; Giannini, C. A new "one-pot" synthesis of hydrazides by reduction of hydrazones. *Tetrahedron* **2003**, *59*, 7733–7742. [CrossRef]
7. Khurana, J.M.; Kandpal, B.M.; Sharma, P.; Gupta, M. A novel method of reduction of >C=N-group in hydrazones, phenylhydrazones, azines, and tosylhydrazones by Mg–methanol. *Monatshefte Chem.* **2015**, *146*, 187–190. [CrossRef]
8. Desai, S.R.; Laddi, U.V.; Benur, R.B.; Bennur, S.C. Synthesis and Antimicrobial Activities of Some New Azetidin-2-ones and Thiazolidin-4-ones. *Indian J. Pharm. Sci.* **2011**, *73*, 478–482. [PubMed]
9. El-masry, A.H.; Fahmy, H.H.; Abdelwahed, S.H.A. Synthesis and Antimicrobial Activity of Some New Benzimidazole Derivatives. *Molecules* **2000**, *5*, 1429–1438. [CrossRef]
10. Mariappan, G.; Korim, R.; Joshi, N.M.; Alam, F.; Hazarika, R.; Kumar, D.; Uriah, T. Synthesis and biological evaluation of formazan derivatives. *J. Adv. Pharm. Technol. Res.* **2010**, *1*, 396–400. [CrossRef] [PubMed]
11. Sah, P.; Bidawat, P.; Seth, M.; Gharu, C.P. Synthesis of formazans from Mannich base of 5-(4-chlorophenyl amino)-2-mercapto-1,3,4-thiadiazole as antimicrobial agents. *Arabian J. Chem.* **2014**, *7*, 181–187. [CrossRef]
12. Rollas, S.; Küçükgüzel, S.G. Biological Activities of Hydrazone Derivatives. *Molecules* **2007**, *12*, 1910–1939. [CrossRef] [PubMed]
13. Melnyk, P.; Leroux, V.; Sergheraert, C.; Grellier, P. Design, synthesis and in vitro antimalarial activity of an acylhydrazone library. *Bioorg. Med. Chem. Lett.* **2006**, *16*, 31–35. [CrossRef] [PubMed]
14. El-Faham, A.; Farooq, M.; Khattab, S.N.; Elkayal, A.M.; Ibrahim, M.F.; Abutaha, N.; Wadaan, M.A.; Hamed, E.A. Synthesis and Biological Activity of Schiff Base Series of Valproyl, N-Valproyl Glycinyl, and N-Valproyl-4-aminobenzoyl Hydrazide Derivatives. *Chem. Pharm. Bull.* **2014**, *62*, 591–599. [CrossRef]
15. Vicini, P.; Incerti, M.; LaColla, P.; Loddo, R. Anti-HIV evaluation of benzo[*d*]isothiazole hydrazones. *Eur. J. Med. Chem.* **2009**, *44*, 1801–1807. [CrossRef] [PubMed]
16. El-Sabbagh, O.I.; Rady, H.M. Synthesis of new acridines and hydrazones derived from cyclic β-diketone for cytotoxic and antiviral evaluation. *Eur. J. Med. Chem.* **2009**, *44*, 3680–3688. [CrossRef] [PubMed]

17. Kumar, D.; Judge, V.; Narang, R.; Sangwan, S.; Clercq, E.D.; Balzarini, J.; Narasimhan, B. Benzylidene/2-chlorobenzylidene hydrazides: Synthesis, antimicrobial activity, QSAR studies and antiviral evaluation. *Eur. J. Med. Chem.* **2010**, *45*, 2806–2816. [CrossRef] [PubMed]
18. Čačić, M.; Molnar, M.; Bojan Šarkanj, B.; Has-Schön, E.; Rajković, V. Synthesis and Antioxidant Activity of Some New Coumarinyl-1,3-Thiazolidine-4-ones. *Molecules* **2010**, *15*, 6795–6809. [CrossRef] [PubMed]
19. Rajitha, G.; Saideepa, N.; Praneetha, P. Synthesis and evaluation of N-(α-benzamido cinnamoyl) aryl hydrazone derivatives for anti-inflammatory and antioxidant activities. *Indian J. Chem.* **2011**, *50B*, 729–733.
20. Alafeefy, A.M.; Bakht, M.A.; Ganaie, M.A.; Ansarie, M.N.; El-Sayed, N.N.; Awaad, A.S. Synthesis, analgesic, anti-inflammatory and anti-ulcerogenic activities of certain novel Schiff's bases as fenamate isosteres. *Bioorg. Med. Chem. Lett.* **2015**, *25*, 179–183. [CrossRef] [PubMed]
21. Gelb, M.H.; Jain, M.K.; Hanel, A.M.; Berg, O.G. Interfacial enzymology of glycerolipid hydrolases: Lessons from secreted phospholipases A2. *Annu. Rev. Biochem.* **1995**, *64*, 653–688. [CrossRef] [PubMed]
22. Murakami, M.; Kudo, I. Diversity and regulatory functions of mammalian secretory phospholipase A_2s. *Adv. Immunol.* **2001**, *77*, 163–194. [PubMed]
23. Valentin, E.; Lambeau, G. Increasing molecular diversity of secreted phospholipases A(2) and their receptors and binding proteins. *Biochim. Biophys. Acta* **2000**, *1488*, 59–70. [CrossRef]
24. Hanasaki, K.; Arita, H. Phospholipase A_2 receptor: A regulator of biological functions of secretory phospholipase A_2. *Prostaglandins Lipid Mediat.* **2002**, *68–69*, 71–82. [CrossRef]
25. Yagami, T.; Ueda, K.; Askura, K.; Hayasaki-Kajiwara, Y.; Nakazato, H.; Sakaeda, T.; Hata, S.; Kuroda, T.; Takasu, N.; Hori, Y. Group IB secretory phospholipase A_2 induces neuronal cell death via apoptosis. *J. Neurochem.* **2002**, *81*, 449–461. [CrossRef] [PubMed]
26. Peuravuori, H.J.; Funatomi, H.; Nevalainen, T.J. Group I and group II phospholipases A_2 in serum in uraemia. *Eur. J. Clin. Chem. Clin. Biochem.* **1993**, *31*, 491–494. [CrossRef] [PubMed]
27. Rae, D.; Porter, J.; Beechey- Newman, N.; Sumar, N.; Bennett, D.; Hermon-Tylor, J. Type I phospholipase A_2 propeptide in acute lung injury. *Lancet* **1994**, *344*, 1472–1473. [CrossRef]
28. Pruzanski, W.; Vasdas, P.; Stefanski, E.; Urowitz, M.B. Phospholipase A_2 activity in sera and synovial fluids in rheumatoid arthritis and osteoarthritis. Its possible role as a proinflammatory enzyme. *J. Rheumatol.* **1985**, *12*, 211–216. [PubMed]
29. Kitsiouli, E.; Nakos, G.; Lekka, M.E. Phospholipase A_2 subclasses in acute respiratory distress syndrome. *Biochim. Biophys. Acta* **2009**, *1792*, 941–953. [CrossRef] [PubMed]
30. Xu, S.; Chen, C.; Wang, W.-X.; Chen, X.-Y. Crucial role of group IIA phospholipase A2 in pancreatitis-associated adrenal injury in acute necrotizing pancreatitis. *Pathol. Res. Pract.* **2009**, *206*, 73–82. [CrossRef] [PubMed]
31. Abe, T.; Sakamoto, K.; Kamohara, H.; Hirano, Y.; Kuwahara, N.; Ogwa, M. Group II phospholipase A2 is increased in peritoneal and pleural effusions in patients with various types of cancer. *Int. J. Cancer* **1997**, *74*, 245–250. [CrossRef]
32. Garcia-Carreno, F.; Toro, M.N. Classification of Proteases without Tears. *Biochem. Educ.* **1997**, *25*, 161–167. [CrossRef]
33. Krishnaswamy, S. Exosite-driven substrate specificity and function in coagulation. *J. Thromb. Haemost.* **2005**, *3*, 54–67. [CrossRef] [PubMed]
34. Hu, J.; Van den Steen, P.E.; Sang, Q.; Opdenakker, G. Matrix metalloproteinase inhibitors as therapy for inflammatory and vascular diseases. *Nat. Rev. Drug Discov.* **2007**, *6*, 480–498. [CrossRef] [PubMed]
35. Overall, C.M.; Dean, R.A. Degradomics: Systems biology of the protease web. Pleiotropic roles of MMPs in cancer. *Cancer Metastasis Rev.* **2006**, *25*, 69–75. [CrossRef] [PubMed]
36. Dusing, R.; Sellers, F. ACE inhibitors, angiotensin receptor blockers and direct renin inhibitors in combination: A review of their role after the ONTARGET trial. *Curr. Med. Res. Opin.* **2009**, *25*, 2287–2301. [CrossRef] [PubMed]
37. Brik, A.; Wong, C.-H. HIV-1 protease: Mechanism and drug discovery. *Org. Biomol. Chem.* **2003**, *1*, 5–14. [CrossRef] [PubMed]
38. Patick, A.K.; Potts, K.E. Protease Inhibitors as Antiviral Agents. *Clin. Microbiol. Rev.* **1998**, *11*, 614–627. [PubMed]
39. El-Sayed, N.N. E.; AL-Balawi, N.A.; Alafeefy, A.M.; Al-AlShaikh, M.A.; Khan, K.M. Synthesis, Characterization and Antimicrobial Evaluation of some Thiazole-Derived Carbamates, Semicarbazones, Amides and Carboxamide. *J. Chem. Soc. Pak.* **2016**, *38*, 358–368.

40. El-Sayed, N.N.E.; Abdelaziz, M.A.; Wardakhan, W.W.; Mohareb, R.M. The Knoevenagel reaction of cyanoacetylhydrazine with pregnenolone, Synthesis of thiophene, thieno[2,3-*d*]pyrimidine, 1,2,4-triazole, pyran and pyridine derivatives with anti-inflammatory and anti-ulcer activities. *Steroids* **2016**, *107*, 98–111. [CrossRef] [PubMed]
41. Wardakhan, W.W.; El-Sayed, N.N. New approaches for the synthesis of 1,3,4-thiadiazole and 1,2,4-triazole derivatives with antimicrobial activity. *Phosphorous Slufur Silicon Relat. Elem.* **2009**, *184*, 790–804. [CrossRef]
42. Alafeefy, A.M.; Awaad, A.S.; Abdel-Aziz, H.A.; El-Meligy, R.M.; Zain, M.E.; Al-Outhman, M.R.; Becha, A.B. Synthesis and biological evaluation of certain 3-substituted benzylideneamino-2-(4-nitrophenyl) quinazolin-4(3*H*)-one derivatives. *J. Enzyme Inhib. Med. Chem.* **2015**, *30*, 270–276. [CrossRef] [PubMed]
43. Vanden Berghe, D.A.; Vlietinck, A.J. Screening methods for antibacterial and antiviral agents from higher plants. In *Methods in Plant Biochemistry-Assay for Bioactivity*; Dey, P.M., Harborne, J.B., Hostettman, K., Eds.; Academic Press: London, UK, 1991; pp. 47–69.
44. Mouchlis, V.D.; Magrioti, V.; Barbyianni, E.; Cermak, N.; Oslund, R.C.; Mavromoustakos, T.M.; Gelb, M.H.; Kokotos, G. Inhibition of secreted phospholipases A2 by 2-oxoamides based on α-amino acids: Synthesis, in vitro evaluation and molecular docking calculations. *Bioorg. Med. Chem.* **2011**, *19*, 735–743. [CrossRef] [PubMed]
45. Jany, K.-D.; Lederer, G.; Maye, B. Amino acid sequence of proteinase K from the mold *Tritirachium album* Limber: Proteinase K—A subtilisin-related enzyme with disulfide bonds. *FEBS Lett.* **1986**, *199*, 139–144. [CrossRef]
46. Milewski, S. Glucosamine-6-phosphate synthase—The multi-facets enzyme. *Biochim. Biophys. Acta* **2002**, *1597*, 173–192. [CrossRef]
47. Durand, P.; Golinelli-Pimpaneau, B.; Mouilleron, S.; Badet, B.; Badet-Denisot, M.A. Highlights of glucosamine-6P synthase catalysis. *Arch. Biochem. Biophys.* **2008**, *474*, 302–317. [CrossRef] [PubMed]
48. Hollenhorst, M.A.; Ntai, I.; Badet, B.; Kelleher, N.L.; Walsh, C.T. A Head-to-Head Comparison of Eneamide and Epoxyamide Inhibitors of Glucosamine-6-Phosphate Synthase from the Dapdiamide Biosynthetic Pathway. *Biochemistry* **2011**, *50*, 3859–3861. [CrossRef] [PubMed]
49. Wojciechowski, M.A.; Milewski, S.; Mazerski, J.; Borowski, E. Glucosamine-6-phosphate synthase, a novel target for antifungal agents. Molecular modelling studies in drug design. *Acta Biochim. Pol.* **2005**, *52*, 647–653. [PubMed]
50. De Araújo, A.L.; Radvanyi, F. Determination of phospholipase A_2 activity by a colorimetric assay using a pH indicator. *Toxicon* **1987**, *25*, 1181–1188. [CrossRef]
51. Kunitz, M.J. Crystalline soyabean trypsin inhibitor II. General properties. *Gen. Physiol.* **1947**, *30*, 291–310. [CrossRef]

Sample Availability: Samples of the compounds are available from the authors.